



저작자표시-비영리-변경금지 2.0 대한민국

이용자는 아래의 조건을 따르는 경우에 한하여 자유롭게

- 이 저작물을 복제, 배포, 전송, 전시, 공연 및 방송할 수 있습니다.

다음과 같은 조건을 따라야 합니다:



저작자표시. 귀하는 원저작자를 표시하여야 합니다.



비영리. 귀하는 이 저작물을 영리 목적으로 이용할 수 없습니다.



변경금지. 귀하는 이 저작물을 개작, 변형 또는 가공할 수 없습니다.

- 귀하는, 이 저작물의 재이용이나 배포의 경우, 이 저작물에 적용된 이용허락조건을 명확하게 나타내어야 합니다.
- 저작권자로부터 별도의 허가를 받으면 이러한 조건들은 적용되지 않습니다.

저작권법에 따른 이용자의 권리는 위의 내용에 의하여 영향을 받지 않습니다.

이것은 [이용허락규약\(Legal Code\)](#)을 이해하기 쉽게 요약한 것입니다.

[Disclaimer](#)

Thesis for the Degree of Master of Physics

Movement of Potassium Ions in channel KcsA
using a Molecular Dynamics Simulation



by

Myo Jeong Kim

Department of Physics

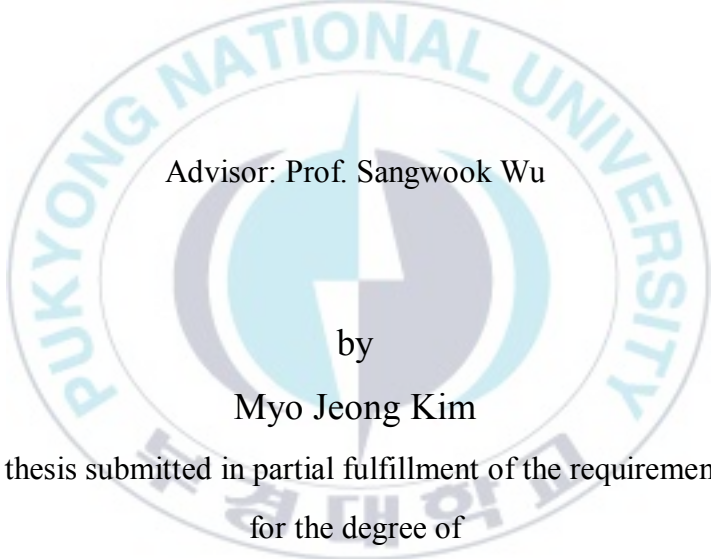
The Graduate School

Pukyong National University

August 2019

Movement of Potassium Ions in channel KcsA
using a Molecular Dynamics Simulation

분자 동역학을 이용한 칼륨 채널
KcsA 내부의 이온 움직임 분석



Advisor: Prof. Sangwook Wu

by

Myo Jeong Kim

A thesis submitted in partial fulfillment of the requirements
for the degree of

Master of Physics

in Department of Physics, The Graduate School,
Pukyong National University

August 2019

Movement of Potassium Ions in channel KcsA using a Molecular Dynamics Simulation

A thesis

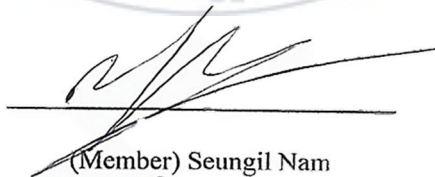
by

Myo Jeong Kim

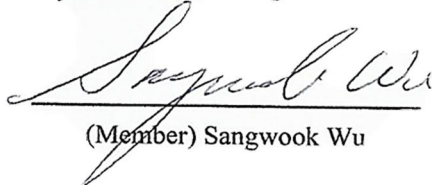
Approved by



(Chairman) Jae-Won Jang



(Member) Seungil Nam



(Member) Sangwook Wu

August 2019

Content

I. Introduction	1
1. Protein	1
1.1. Protein and amino acids	1
2. Ion Channel	4
2.1. Ion Channel	4
II. Methods	9
1. Molecular Dynamics Simulation	9
1.1. Force field	10
1.1.1. Bond stretching	13
1.1.2. Angle bending	13
1.1.3. Bond rotation	14
1.1.4. Non-bonded interaction	15
1.1.5. Particle Mesh Ewald	16
2. Molecular Dynamics Simulation and Ensemble	21
2.1. NVT ensemble	21
2.2. NPT ensemble	23
2.3. Verlet algorithm	24
III. Results and Discussion	26
1. Movement of Potassium Ions inside KcsA	27
1.1. Structure of KcsA	27

1.2. RMSD of each helix.....	29
1.3. Distance between selectivity filter and potassium ion.....	33
1.4. Correlation map with ion change	38
1.5. Movement and change of KcsA internal potassium and water molecules.....	42
IV. Conclusions.....	44
Reference.....	46



List of figure

Figure I-1. General structure of amino acids.....	2
Figure I-2. Twenty different types of side chains (20 amino acids) [1]	2
Figure I-3. 4 levels of protein structure [1]	3
Figure I-4. Voltage-gated ion channel.....	5
Figure I-5. PDB structure 1K4C. Salmon is chain A, green is chain B, yellow is chain C and purple is potassium ion [6].....	7
Figure II-1. Schematic representation of the four components to a molecular mechanics force field.....	12
Figure II-2. The periodic box in the Ewald method. The length of box is L.....	17
Figure III-1. Structure of potassium channel KcsA (a) side view (b) top view.....	27
Figure III-2. RMSD of potassium channel (a) Selectivity filter (b) Pore helix (c) Inner Helix (d) Outer Helix (e) Whole backbone (f) Comparison of all RMSD.....	29
Figure III-3. Distances of three potassium ions (K1, K2, and K3) with respect to Thr75, Val76, Gly77, Tyr78, and Gly79 inside selectivity filter.....	33
Figure III-4. Correlation map between the two KcsA structures at 43.38 ns and 43.44 ns.....	36
Figure III-5. Correlation map between the two KcsA structures at (a) 43.38 ns, (b) 43.44 ns, (c) the difference between (a) and (b).....	38
Figure III-6. Movement and change of KcsA internal potassium and water molecules. Snapshots are taken at (a) 3.6 ns, (b) 17.3 ns, (c) 43.38 ns, and (d) 43.44 ns.....	42

분자 동역학을 이용한 칼륨 채널 KcsA 내부 이온의 움직임 분석

김 묘 정

부경대학교 대학원 물리학과

요약

전압에 의존하는 이온 채널은 이온 전도를 통해, 세포막 전압의 변화에 반응한다. 이러한 이온에는 나트륨, 칼륨 및 칼슘 이온 등이 포함된다. 또한 이온 채널은 신경과 근육의 활동에 기초가 되기 때문에 그 구조와 동역학을 관측하는 것이 생물학적으로 의미가 크다. 그 중 칼륨 채널의 단백질의 구조 및 이온이 주어진 환경에서 어떤 변화를 보이는지 확인하기 위하여 분자 동역학을 실시하였다. 이 방법은 칼륨 이온 채널에 대해 진행되었다. 본 논문에서는 특히 KcsA 채널의 움직임 및 내부 이온을 관측하였다. 이 연구에서 주어진 환경은 첫 째, 일반적인 체내 칼륨 농도 보다 2배로 높고 둘 째, 세포막에 전압을 인가하지 않았다. 이렇게 분자 동역학으로부터 얻어진 결과를 통해 실제 칼륨 이온 채널의 움직임을 예측하고 그 원동력을 자세히 알아볼 수 있다.

I. Introduction

1. Protein

1.1. Protein and amino acids

1.1.1. Amino acids

All proteins are polymers of amino acids. Each amino acid is attached to another amino acid by a covalent bond. According to the R group [1, 2, 3], 20 amino acids are known and amino acids can be classified based on the characteristic. There are shown in Figure I-1 and Figure I-2. .

Based on growth or nitrogen balance, amino acids are classified as nutritionally essential or nonessential for animals and humans, i.e. purity of proteins throughout the body. Nutritional essential amino acids can't be made by cells and must be obtained through the diet. Dietary essentiality of some amino acids (e.g., arginine, glycine, proline, and taurine) rely on species and developmental stage.

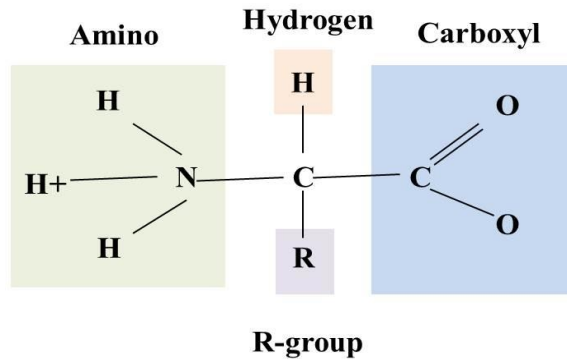


Figure I-1. General structure of amino acids

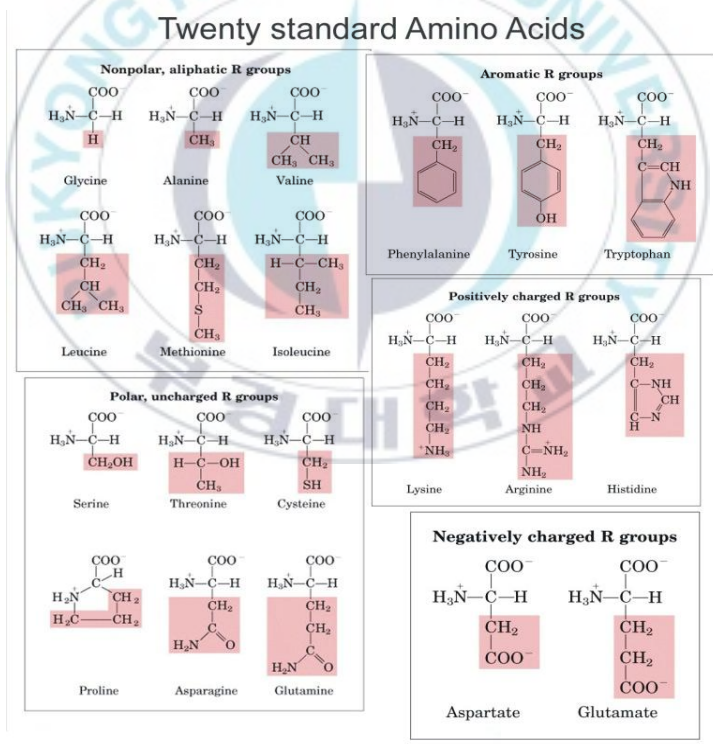


Figure I-2. Twenty different types of side chains (20 amino acids)[1]

1.1.2. Protein

Protein structure is described by four different levels known as primary, secondary, tertiary, and quaternary structure [1]. First, the primary structure is a polymer chain consisting of the sequence of amino acids. Protein secondary structure refers to the hydrogen bond patterns. The two patterns are the alpha-helix and the beta-sheets. Tertiary structure refers to the overall folding of the secondary structures in a form that can perform simple functions. For example, Myoglobin are formed from alpha-helices. Quaternary structure is the arrangement of more than one protein to form the overall structure of the protein. Figure I-3 shows four levels of protein structure.

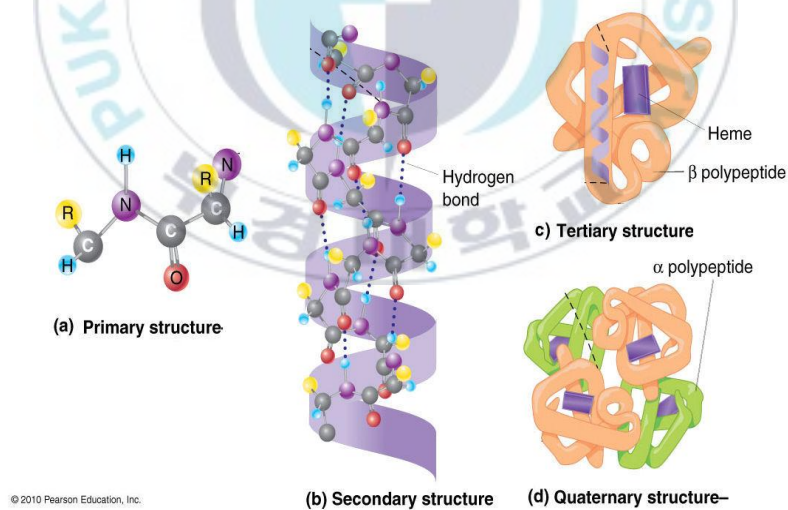


Figure I-3. 4 levels of protein structure [1]

2. Ion Channel

2.1. Ion Channel

2.1.1. Ion Channel

Some cells, often called stimulant cells, generate electrical signals. There are many kinds of exciting cells, such as neurons, muscle cells and touch receptor cells, but all of them use ion channel receptors to convert chemical or mechanical messages into electrical signals. Like all cells, stimulant cells maintain a different amount of ionic concentration than those present in an extracellular environment. All of these concentration differences produce small potential across plasma membranes. The specialized channel of the plasma membrane is then opened according to the conditions, resulting in ionic movement within or out of the cell, and this movement produces an electrical signal. These ion channels are often called six trans-members. The ion channels are classified according to the opening and closing of the Pore, such as voltage dependence, ligand gate and receptor application.

2.1.1.1. Voltage-gated ion channel

This is because the structure is linked to six helices that penetrate the cell membrane. The names of each column are S1, S2, S3, S4, S5 and S6, respectively. Specifically, it detects voltages from S1 to S4 and changes the structure of proteins that form ion channels. In addition, S5 and S6 are areas where the ion actually passes through and are related to the function of ion channels, such as selection filters. The opening and closing of this channel are changed to a three-dimensional form by voltage. There are also ball and chain models. Twenty amino acids form a ball and close the ion channel by attaching to a flexible chain. The ions move when the channel is opened, and when the membrane potential is positive, the channel closes when the ball tries to go out of the cytoplasm. Thus, The longer the chain, the longer the opening time.

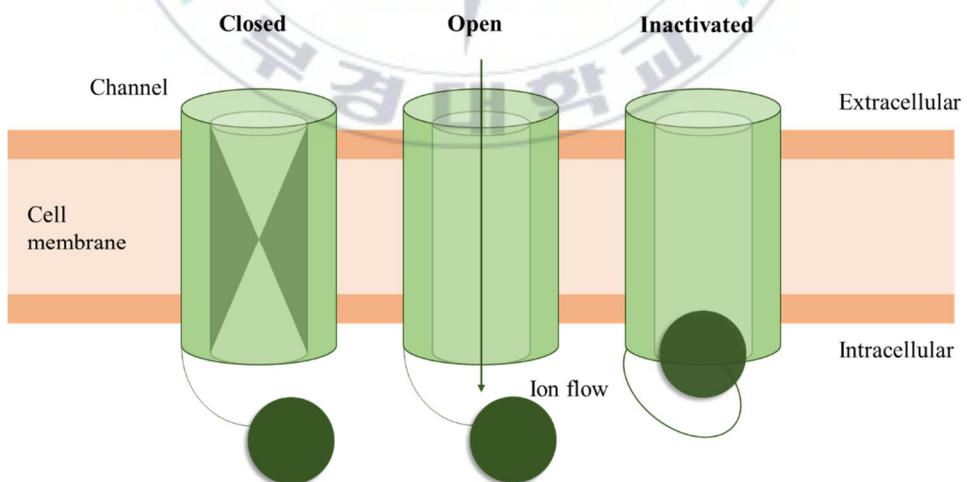


Figure I-4. Voltage-gated ion channel

2.1.2. Potassium ion channel

The interaction between the major residue of the potassium channel and the potassium ion has the option for passive diffusion of potassium ions. The potassium channel filter also selectively penetrates potassium ions between different ions of similar size from dehydration under certain potentials. The effect of potassium ion conduction is mostly to counter environmental changes in terms of electrochemical potential and concentration changes. Recently, the high-resolution structure of the potassium channel confirmed that there are two gates formed in a spiral. These gates control ion selectivity through the interaction between potassium ion and pore interface.

One gate is located in a separate spiral, with an optional filter on the spiral. Located at the membrane intersection, this gate responds to voltage potential changes, and the other gate acts as a selection filter when the channel is open. The selection filter spiral consists of a TVGYG sequence, a key channel motif that accurately induces potassium ions [4, 5, 6, 7]. Stabilize the negative potassium ion of the carbonyl oxygen atom in the amino acid located inside the selective filter to the anode. The distance between carbonyl oxygen atoms is about the same as the diameter of potassium ions, so only potassium ions can pass through this [8, 9].

2.1.3. KcsA

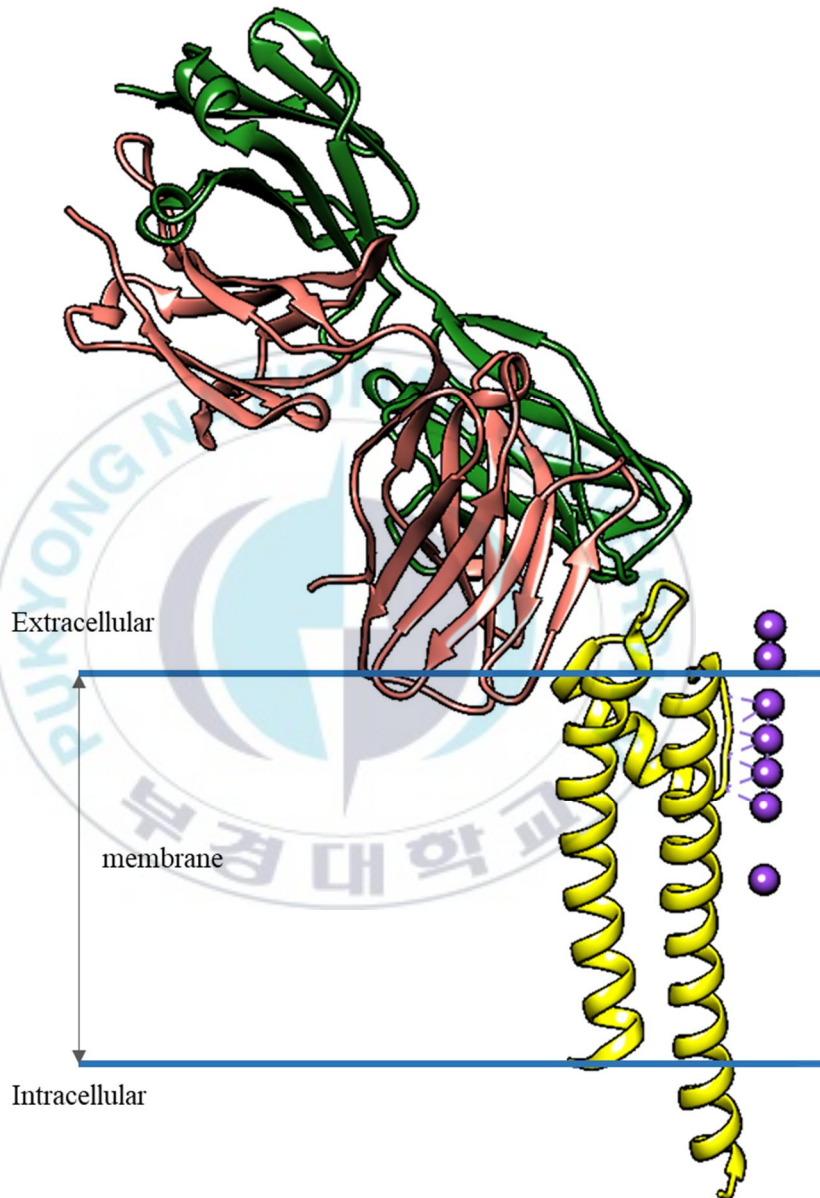


Figure I-5. PDB structure 1K4C. Salmon is chain A, green is chain B, yellow is chain C and purple is potassium ion [6]

KcsA(*K channel of streptomyces A*) is a prokaryotic potassium channel in *Streptomyces* lipids. The KcsA structure (PDB ID: 1K4C) has a framework for understanding K⁺ channel conduction, which consists of three parts: potassium selectivity, channel gate by pH sensitivity, and voltage gate channel deactivation. 3.2 Å model of KcsA has been produced for resolution, arranged around the central pore with the spiral of each subunit facing the inner axis and the other facing outward [6]. Based on the energy and electrostatic calculations made for modeling pore areas, evidence of the scores of selective filters by the 2 K⁺ atoms during the transport process emerged. Continued investigations into KcsA's various opening and closing [10, 11, 12], inactivity and active compliance by other methods, such as ssNMR, provided a lot of insight into the channel structure and the power to gate the switch from channel inactivity to an electric furnace. The main chain carbonyl oxygen atom that forms the selective filter is fixed in a precise position that can replace the water molecule in the watery shell of potassium ions [5].

II. Methods

In this study, we investigated the potassium in the KcsA channel [13, 14, 15, 16, 17, 18]. We performed molecular dynamics (MD) simulation to observe the moving of potassium ion with high concentration system [19, 20, 21].

1. Molecular Dynamics Simulation

Molecular dynamics (MD) simulations is one of the effective methods to study the dynamics of biological molecules, such as protein, DNA, and lipid [22, 23, 24, 25]. The basic principle of MD simulation is to solve on newton's equation.

$$\frac{d^2x_i}{dt^2} = \frac{F_{x_i}}{m_i} \quad (2.1)$$

This equation means the motion of a particle of mass m_i along one coordinate (x_i) with F_{x_i} being the force on the particle in that direction. When we solve the differential equation, we can obtain trajectory that specifies how the positions and velocities of the particles in the system vary with time.

1.1. Force field

MD simulation requires the definition of potential function (called the *force field*) to perfect the simulation from the relation of

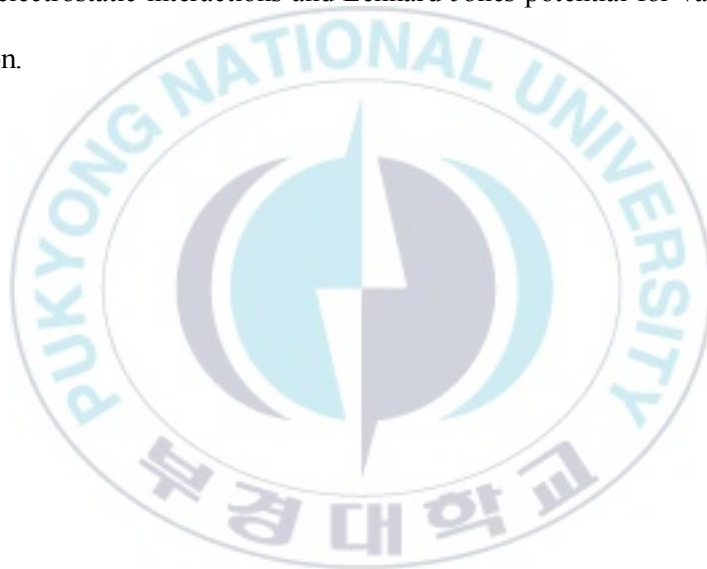
$$\mathbf{F} = -\frac{dU}{d\mathbf{r}} \quad (2.2)$$

The potential function is composed of four components such as bond stretching, angle bending, bond rotation (torsion) and non-bonded interaction (Figure II-1) [25], The three components except non-bonded interaction corresponds to bonded-part of potential function. These four components are associated with the “deviation” for bonds and angles from their reference or equilibrium values. The potential is given as

$$\begin{aligned} U(\mathbf{r}^N) = & \sum_{bonds} \frac{k_1}{2} (l_i - l_{i,0})^2 \\ & + \sum_{angles} \frac{k_1}{2} (\theta_i - \theta_{i,0})^2 \\ & + \sum_{torsions} \frac{B_n}{2} (1 + \cos(n\omega - \gamma)) \\ & + \sum_{i=1}^N \sum_{j=i+1}^N (4\epsilon_{ij} \left[\left(\frac{\sigma_{ij}}{r_{ij}} \right)^{12} - \left(\frac{\sigma_{ij}}{r_{ij}} \right)^6 \right] + \frac{q_i q_j}{4\pi\epsilon_0 r_{ij}}) \end{aligned} \quad (2.3)$$

where $U(\mathbf{r}^N)$ means potential energy. It is a function of the position \mathbf{r} of N particles. The first term provides information of interaction between pair bonded atoms. l_i is bond length, $l_{i,0}$ is reference bond length value. The second term

provides information of all the angle in the molecule. The first and second term adopts harmonic potential. The third term models dihedral angles, rotation of bond. The first, second, and third term are bonded part in potential function U . The fourth term is non-bonded part. This term calculates the pairs of atoms (i and j) that re in different molecules or that are in the same molecule but separated by at least three bonds. The non-bonded part of this equation is composed of Coulomb potential term for electrostatic interactions and Lennard-Jones potential for van der Waals interaction.



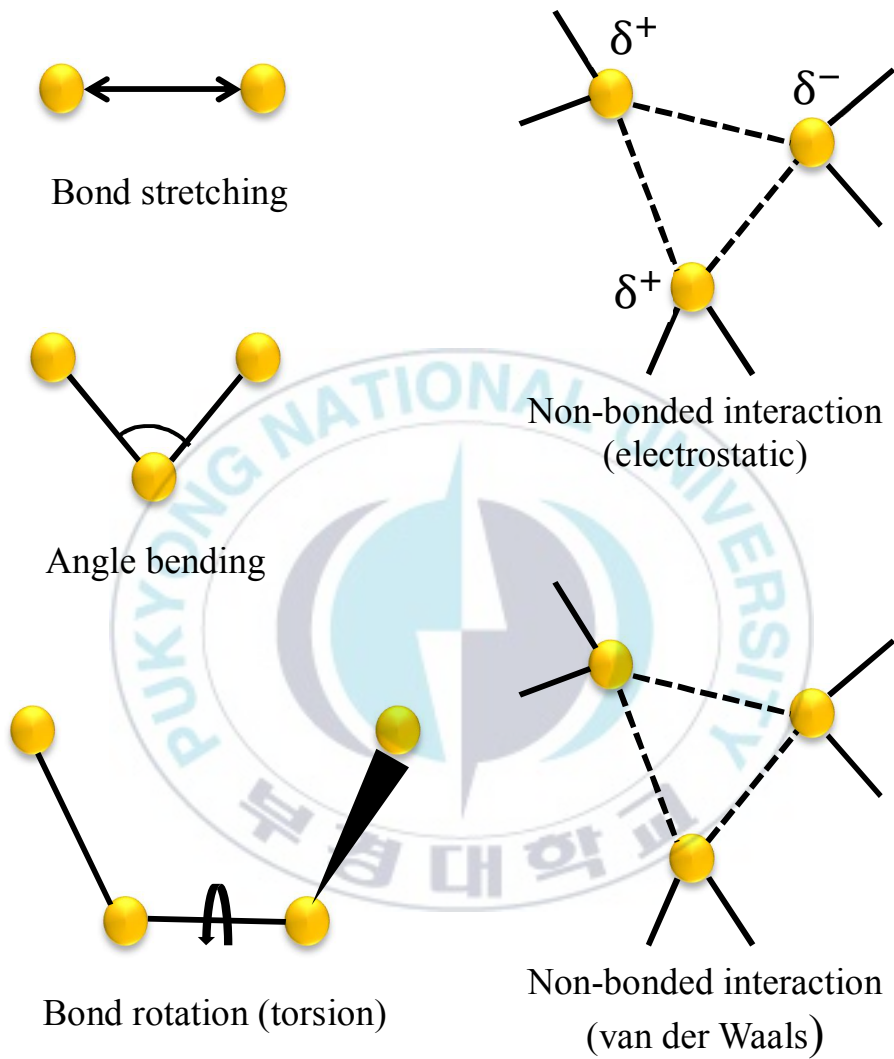


Figure II-1. Schematic representation of the four components to a molecular mechanics force field

1.1.1. Bond stretching

The first term of equation (2.3) means bond stretching. The most elementary approach is to use a Hooke's law, in which the energy varies with the square of the displacement from the reference bond length l_0 .

$$v(l) = \frac{k}{2}(l - l_0)^2 \quad (2.4)$$

The reference bond length l_0 is the value that bond adopts when all other terms in the force field are set to zero.

1.1.2. Angle bending

The second term of equation (2.3) describes angle bending. The deviation of angles from their reference values is also frequently described as Hooke's law or harmonic potential.

$$v(\theta) = \frac{k}{2}(\theta - \theta_0)^2 \quad (2.5)$$

The contribution of each angle is characterized by a force constant and reference value.

1.1.3. Bond rotation

The third term of equation (2.3) is torsional (dihedral angle) part. Bond stretching and angle bending term require substantial energies to cause deformations from their reference values. The existence of barriers to rotation about chemical bonds is fundamental to understanding the structural properties of molecules. For example, torsional term have three maximum energies and three minimum energies for ethylene. The eclipsed conformation has maximum energies for ethylene. On the other hand, staggered conformations have minimum energies. The potential for the bond rotation is given as

$$v(\omega) = \sum_{n=0}^N \frac{V_n}{2} [1 + \cos(n\omega - \gamma)] \quad (2.6)$$

where V_n is torsion fore constant. A multiplicity of function n is the number of minimum points when bond is rotated through 360° and ω is dihedral angle. The phase factor γ determines where the torsion angle passes through its minimum value.

1.1.4. Non-bonded interaction

The last term of equation (2.3) is non-bonded term. The non-bonded interactions do not depend upon a specific bonding relationship between atoms. They are ‘through-space’ interactions. The non-bonded term is Coulomb potential for electrostatic interactions and Lennard-Jones potential for van der Waals interactions. We discuss electrostatic interactions. The electrostatic interaction between two molecules (or between different part of the same molecule) is obtained as a sum of interactions between pairs of point charges,

$$v = \sum_{i=1}^{N_A} \sum_{j=1}^{N_B} \frac{q_i q_j}{4\pi\epsilon_0 r_{ij}} \quad (2.7)$$

where N_A and N_B are the numbers of point charges in the molecule.

The van der Waals interaction is consists of the all the non-bonded interactions between atoms (or molecules) that are not covered by the electrostatic interaction. These interactions are expressed as Lennard-Jones potential,

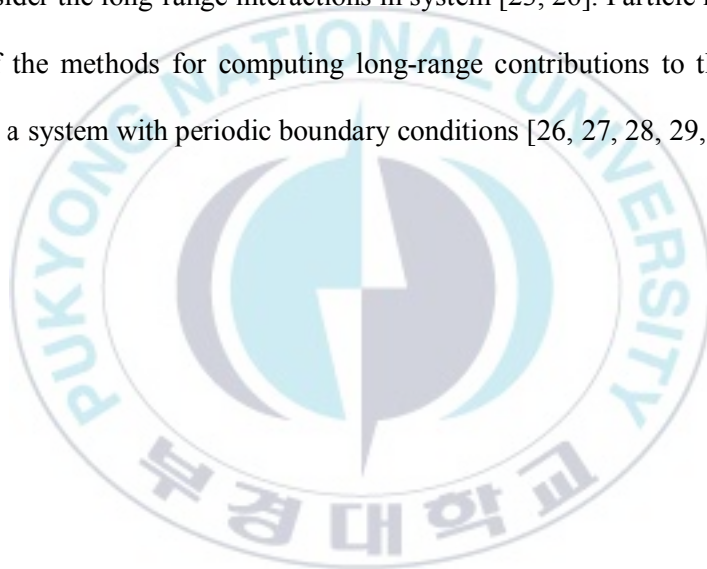
$$v(r_{ij}) = \sum_{i=1}^N \sum_{j=i+1}^N 4\epsilon_{ij} \left[\left(\frac{\sigma_{ij}}{r_{ij}} \right)^{12} - \left(\frac{\sigma_{ij}}{r_{ij}} \right)^6 \right] \quad (2.8)$$

Where r_{ij} is the distance between the atom i and j , σ is the collision diameter (the separation for which the energy is zero) and ϵ is the energy depth which shows the bonding of particles. The r^{-12} term is the strong repulsive at short

ranges due to overlapping electron orbitals, and the r^{-6} term describes a weak attraction between individual molecules at long range. It goes to infinity as the distance goes to zero.

1.1.5. Particle Mesh Ewald

We consider the long-range interactions in system [23, 26]. Particle mesh Ewald is one of the methods for computing long-range contributions to the potential energy in a system with periodic boundary conditions [26, 27, 28, 29, 30].



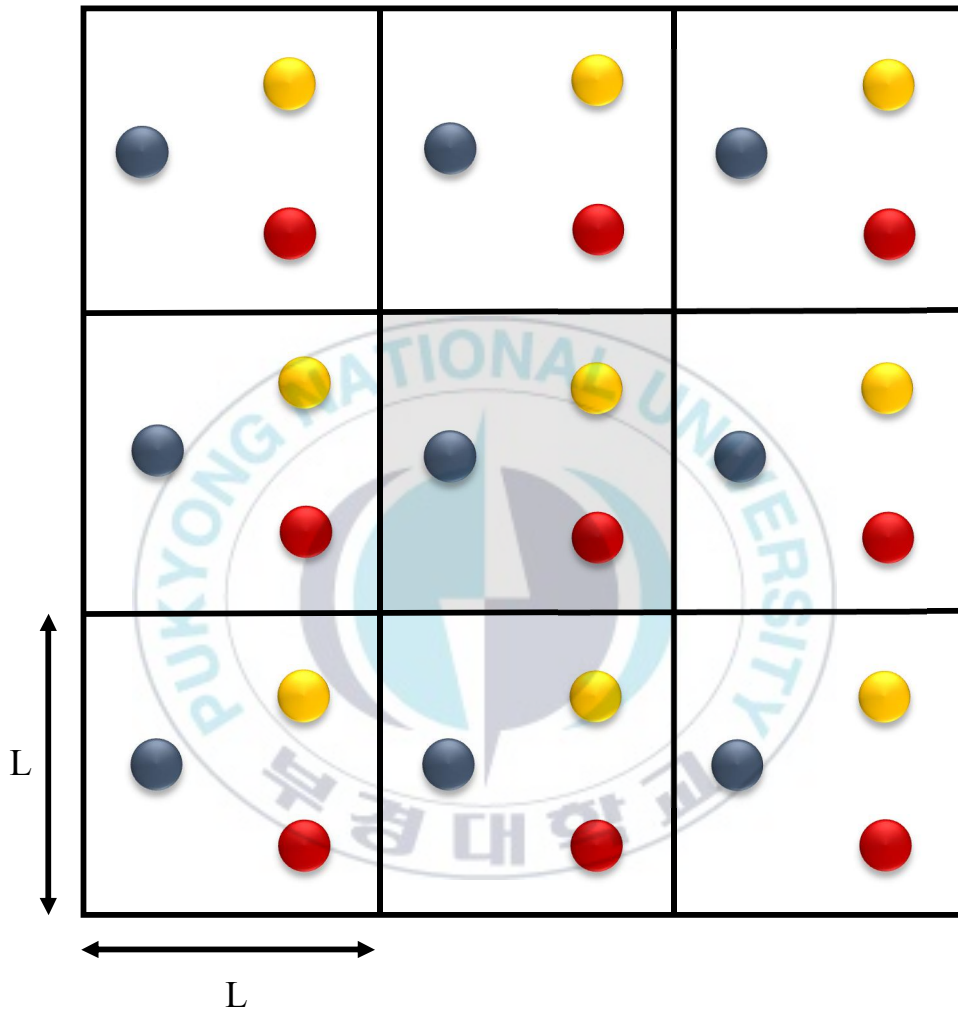


Figure II-2. The periodic box in the Ewald method. The length of box is L

Let us first consider a system consisting of positively and negatively charged particles. The system is electrically neutral, $\sum_i q_i = 0$. These particles are assumed to be located in a cube with diameter L and the system has periodic boundary conditions as shown in (Fig II-2). The total number of particles in the fundamental simulation box (the unit cell) is N . All particles repel each other at sufficiently short distances. In this periodic condition, the Coulomb potential energy is given as,

$$u_{\text{coul}} = \frac{1}{2} \sum_{i=1}^N q_i \phi(r_i) \quad (2.9)$$

where $\phi(r_i)$ is the electrostatic potential at the position of ion i

$$\phi(r_i) = \sum'_{j,n} \frac{q_j}{|\mathbf{r}_{ij} + \mathbf{n}L|} \quad (2.10)$$

A prime on the summation of equation (2.10) indicates that the sum is over all periodic images \mathbf{n} and over all particles j , except $j = i$ if $\mathbf{n} = 0$. r_{ij} is the minimum distance between i and j . In addition, we assume that the compensating charge distribution surrounding an ion i is a Gaussian.

$$\rho_{\text{Gauss}}(r) = -q_i \left(\frac{\alpha}{\pi}\right)^{\frac{3}{2}} \exp(-\alpha r^2) \quad (2.11)$$

where α is determined later by considerations of computational efficiency. It satisfies Poisson's equation.

$$-\nabla^2\phi(\mathbf{r}) = 4\pi\rho(\mathbf{r}) \quad (2.12)$$

We apply the properties of the Poisson equation in Fourier form to compute the electrostatic potential at a point r_i due to a charge distribution $\rho_1(r)$ that consists of a periodic sum of Gaussians.

$$\rho_1(r) = \sum_{j=1}^N \sum_{\mathbf{n}} q_j \left(\frac{\alpha}{\pi}\right)^{\frac{3}{2}} \exp[-\alpha |\mathbf{r} - (\mathbf{r}_j + \mathbf{n}L)|^2] \quad (2.13)$$

We compute the contribution to the potential energy (u_1) due to $\phi_1(r)$. $\phi_1(r)$ is given as

$$\phi_1(r) = \sum_{k \neq 0} \sum_{j=1}^N \frac{4\pi q_j}{k^2} \exp[i\mathbf{k} \cdot (\mathbf{r}_i - \mathbf{r}_j)] \exp\left(-\frac{k^2}{4\alpha}\right) \quad (2.14)$$

Hence

$$u_1 = \frac{1}{2V} \sum_{k \neq 0} \frac{4\pi}{k^2} \rho(\mathbf{k})^2 \exp\left(-\frac{k^2}{4\alpha}\right) \quad (2.15)$$

where V is the volumes of the system. $\rho(k)$ is Fourier transform of charge distribution. For the self-interaction to be corrected, u_{self} should be subtracted from the sum of the real-space and Fourier contributions to the Coulomb energy.

$$u_{\text{self}} = \left(\frac{\alpha}{\pi}\right)^{\frac{1}{2}} \sum_{i=1}^N q_i^2 \quad (2.16)$$

Then, electrostatic potential due to a point charge q surrounded by a Gaussian

with net charge q_i is given as

$$\phi_{\text{short-range}} = \frac{q_i}{r} \operatorname{erfc}(\sqrt{\alpha}r) \quad (2.17)$$

where erfc is complementary error function. The total contribution of the screened Coulomb interactions to the potential energy is then given by

$$u_{\text{short-range}} = \frac{1}{2} \sum_{i \neq j}^N \frac{q_i q_j \operatorname{erfc}(\sqrt{\alpha}r_{ij})}{r_{ij}} \quad (2.18)$$

Finally, the total electrostatic contribution to the potential energy becomes the sum of potential energies u_1 , u_{self} , and $u_{\text{short-range}}$

$$u_{\text{coul}} = \frac{1}{2V} \sum_{k \neq 0} \frac{4\pi}{k^2} |\rho(k)|^2 \exp\left(-\frac{k^2}{4\alpha}\right) - \frac{\left(\frac{\alpha}{\pi}\right)}{2} \sum_{i=1}^N q_i^2 + \frac{1}{2} \sum_{i \neq j}^N \frac{q_i q_j \operatorname{erfc}(\sqrt{\alpha}r_{ij})}{r_{ij}} \quad (2.19)$$

2. Molecular Dynamics Simulation and Ensemble

Molecular dynamics is traditionally performed in the microcanonical ensemble (NVE ensemble: the number of particle (N), volume (V), and the total energy in the system ϵ are constant.). But many experimental measurements are made under conditions of constant temperature and pressure. Therefore, MD simulation adapts the two most common alternative ensembles, isothermal-isobaric ensemble (NPT ensemble: the number of particle (N), pressure (P), and temperature (T) are constant.) and canonical ensemble (NVT ensemble: the number of particle (N), volume (V), and temperature (T) are constant.) [33, 34, 35].

2.1. NVT ensemble

The temperature of the system is related to the time average of the kinetic energy in unconstrained system is given by

$$\langle K \rangle_{\text{NVT}} = \frac{3}{2} N k_B T \quad (2.20)$$

where N is the number of particles. An obvious way to alter the temperature of the system is thus to scale the velocities. The temperature at time t can be expressed as

$$T(t) = \frac{2}{3Nk_B} \sum_{i=1}^N \frac{1}{2} m_i v_i^2 \quad (2.21)$$

where m is mass and v is velocity. If the velocities are multiplied by a factor λ_t , then the associated temperature change can be calculated as follows

$$\Delta T = \frac{2}{3Nk_B} \sum_{i=1}^N \frac{1}{2} m_i (\lambda_t v_i)^2 = \frac{2}{3Nk_B} \sum_{i=1}^N \frac{1}{2} m_i v_i^2 \quad (2.22)$$

$$\Delta T = (\lambda_t^2 - 1)T(t) \quad (2.23)$$

$$\lambda_t = \sqrt{T_{new}/T(t)} \quad (2.24)$$

The simplest way to control the temperature is thus to multiply the velocities at each time step by the factor $\lambda (= \sqrt{\frac{T_{req}}{T_{curr}}})$, where T_{curr} is the current temperature as calculated from the kinetic energy and T_{req} is the desired temperature.

An alternative way to maintain the temperature is to couple the system to an external heat bath, which is fixed at the desired temperature. The bath acts as a source of thermal energy, supplying or removing heat from the system as appropriate. The velocities are scaled at each step, such that the rate of change of temperature is proportional to the difference in temperature between the external heat bath (T_{bath}) and the system.

$$\frac{dT(t)}{dt} = \frac{1}{\tau_t} (T_{bath} - T(t)) \quad (2.25)$$

where τ_t is large, then the coupling will be weak. If τ_t is small, the coupling

will be strong. When the coupling parameter equals the time step ($\tau_t = \delta t$) then the algorithm is equivalent to the simple velocity scaling method. The advantage of this approach enables the system to fluctuate about the desired temperature.

2.2. NPT ensemble

The NPT ensemble is also called isothermal-isobaric ensemble. Many experimental measurements are made under conditions of constant temperature and pressure. A simulation in the NPT ensemble maintains constant pressure by changing the volume of the simulation cell. The amount of volume fluctuation is related to the isothermal compressibility, κ .

$$\kappa = -\frac{1}{V} \left(\frac{\partial V}{\partial P} \right)_T \quad (2.26)$$

Many of the methods used for pressure control are similar to the temperature control method. Thus, the pressure can be maintained at a constant value by simply scaling the volume [31]. An alternative way is to couple the system to a *pressure bath*, as like a temperature bath. The rate of change of pressure is given by

$$\frac{dP(t)}{dt} = \frac{1}{\tau_p} (P_{bath} - P(t)) \quad (2.27)$$

where τ_p is the coupling constant, P_{bath} is the pressure bath, and $P(t)$ is the actual pressure at time t . The volume of the simulation box is scaled by a factor

λ_p , which is equivalent to scaling the atomic coordinates by a factor $\lambda_p^{\frac{1}{3}}$.

$$\lambda_p = 1 - \kappa \left(\frac{\delta t}{\tau_p} \right) (P - P_{bath}) \quad (2.28)$$

The constant κ can be combined with the relaxation constant τ_p as a single constant. The volume can vary during the simulation with the average volume being determined by the balance between the internal pressure of the system and the desired external pressure.

2.3. Verlet algorithm

Verlet algorithm is one of algorithms to integrate Newton's equation, which is the most widely used method for integrating Newton's equation. This algorithm uses the positions and accelerations at time t , and the position from the previous step at time $t - \Delta t$ to calculate the new positions at time $t + \Delta t$.

$$r(t + \Delta t) = r(t) + v(t)\Delta t + \frac{f(t)}{2m}\Delta t^2 + \frac{\Delta t^3}{3!}\ddot{r} + \mathcal{O}(\Delta t^4) \quad (2.29)$$

$$r(t - \Delta t) = r(t) - v(t)\Delta t + \frac{f(t)}{2m}\Delta t^2 - \frac{\Delta t^3}{3!}\ddot{r} + \mathcal{O}(\Delta t^4) \quad (2.30)$$

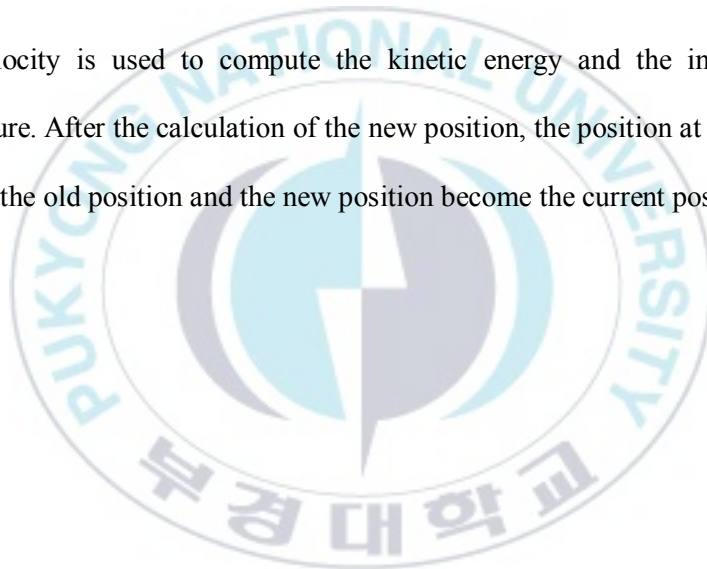
where $f(t)$ is the force at time t . Summing these two equations, a new position $r(t + \Delta t)$ is given as

$$r(t + \Delta t) \approx 2r(t) - r(t - \Delta t) + \frac{f(t)}{m} \Delta t^2 \quad (2.31)$$

where Δt is the time step in MD simulation. Verlet algorithm does not use the velocity to compute the new position. But it derives the velocity from knowledge of the trajectory.

$$v(t) = \frac{r(t + \Delta t) - r(t - \Delta t)}{2\Delta t} + \mathcal{O}(\Delta t^2) \quad (2.32)$$

The velocity is used to compute the kinetic energy and the instantaneous temperature. After the calculation of the new position, the position at time $t - \Delta t$ becomes the old position and the new position become the current position.



III. Results and Discussion

We investigate the structure of channel proteins and the ion motion in them predicted by molecular mechanics. The KcsA is conducted only in environments with no voltage and a concentration of 400 mM of KCl [32]. First, we confirm the stability of the segment and then observe the movement of ions through internal pores. Three potassium ions and two water molecules pass through the selective filter alternatively.

The analysis of result is reported as follows.

- Structure of potassium channel
- RMSD of each helix
- Distance of selective filter and potassium ion
- Correlation map with ion change
- Movement and change of KcsA internal potassium and water molecules

1. Movement of Potassium Ions inside KcsA

1.1. Structure of KcsA

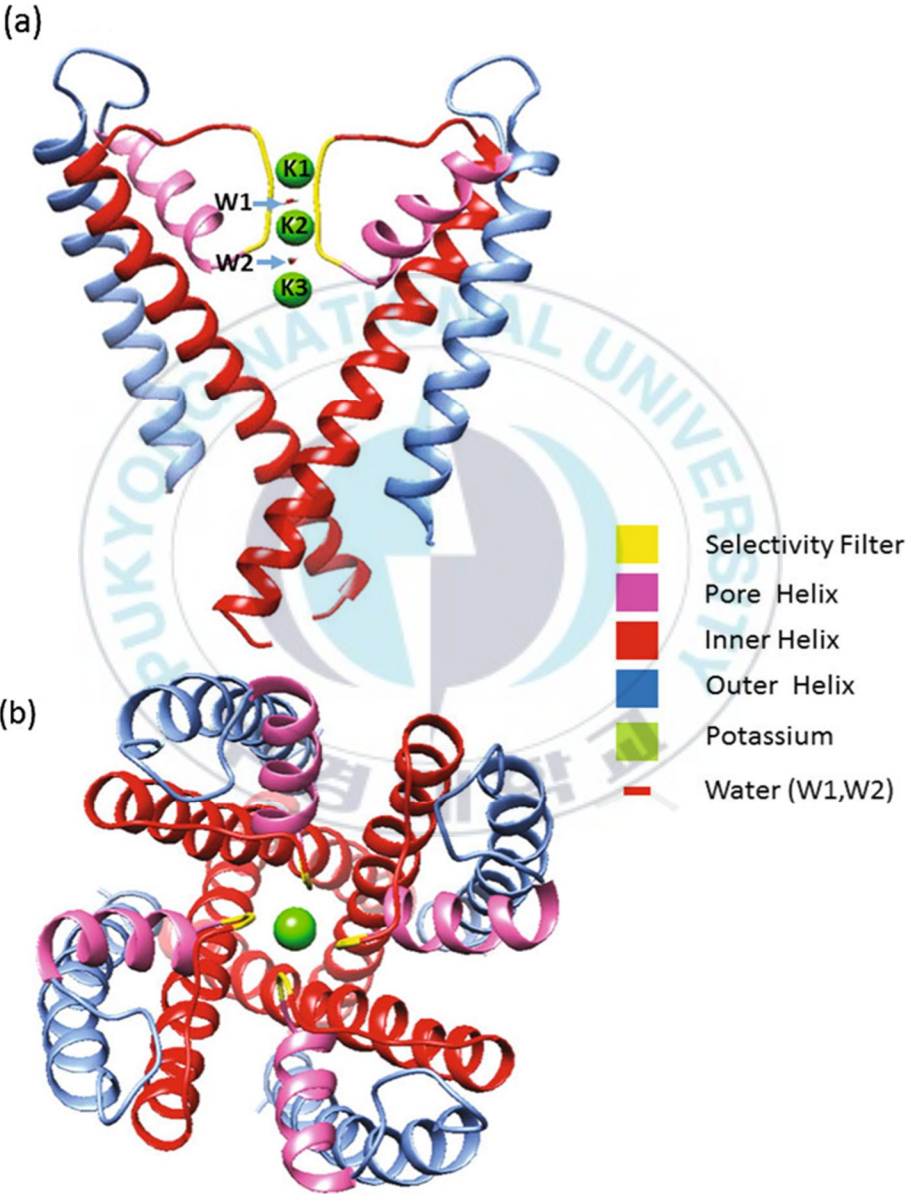
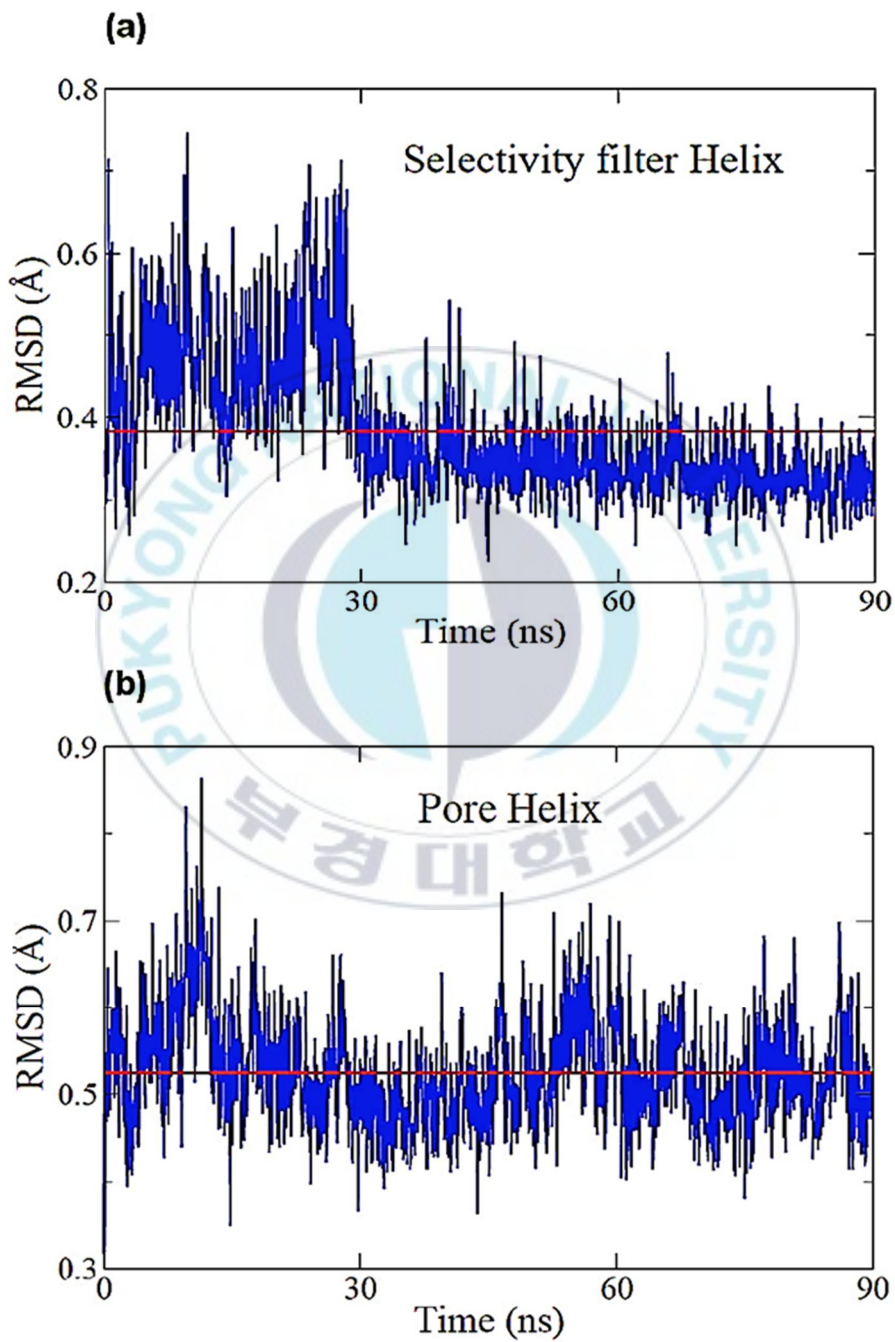


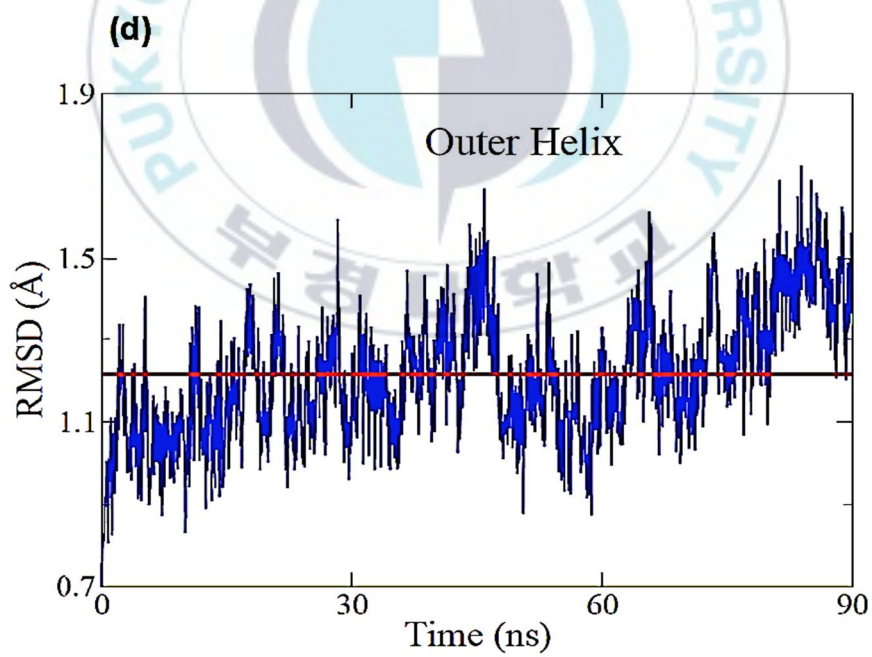
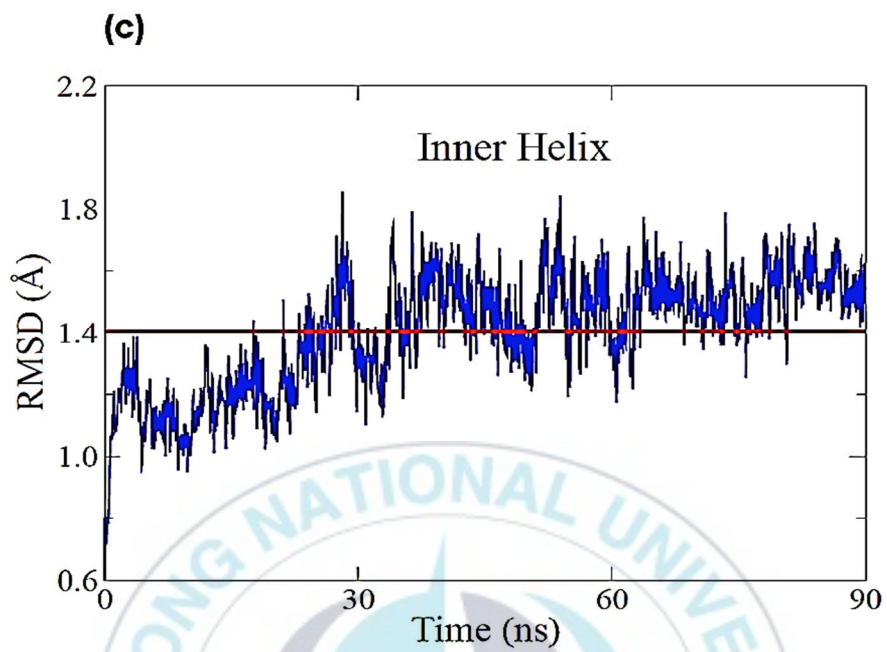
Figure III-I. Structure of potassium channel KcsA (a) side view (b) top view

The KcsA has a funnel-shaped figure. It is made up of four chains and has 22 to 124 residues per chain. It also corresponds to a membrane protein located in the cell membrane. KcsA is the same size as the ordinary cell membrane.

A selectivity filter with the most essential function is 75 to 79 residues, with O that placed towards the center of the pore. A pore helix forms the pore. This pore helix consists of 62 to 75 residues. An outer helix consists of 22 to 62 residues, the inner helix has 79 to 124 residues. Figure III-1 (a) shows how potassium passes through between the selectivity filter. Five oxygens per each chain stabilize potassium ions in channel [33, 34]. Water and potassium ions pass through alternatively between selectivity filter as equivalent to the movement of traditional potassium ions. Figure III-1 (b) shows all four chains are symmetrical. It can also show that potassium ions can pass through the selectivity filter since the pore has a suitable space.

1.2. RMSD of each helix





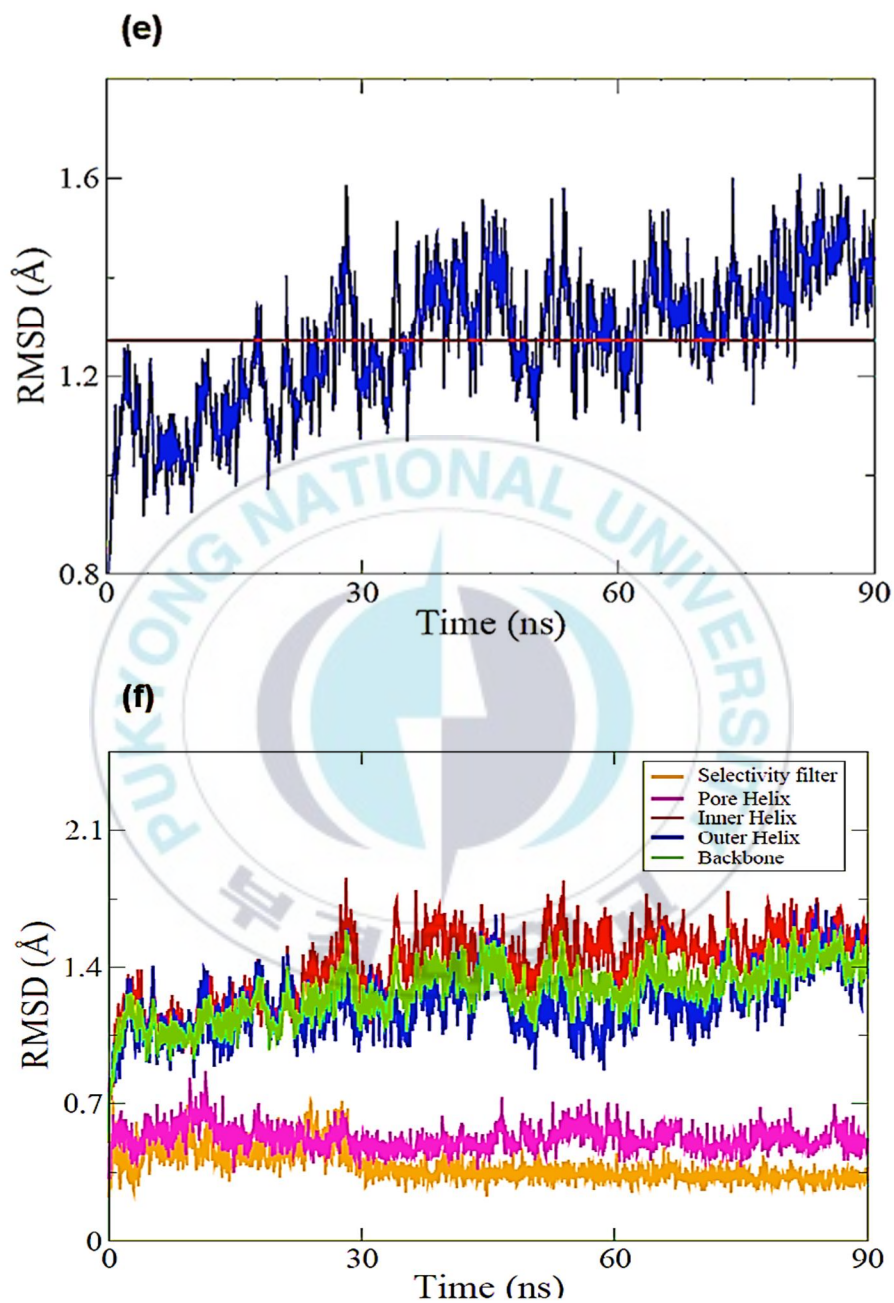
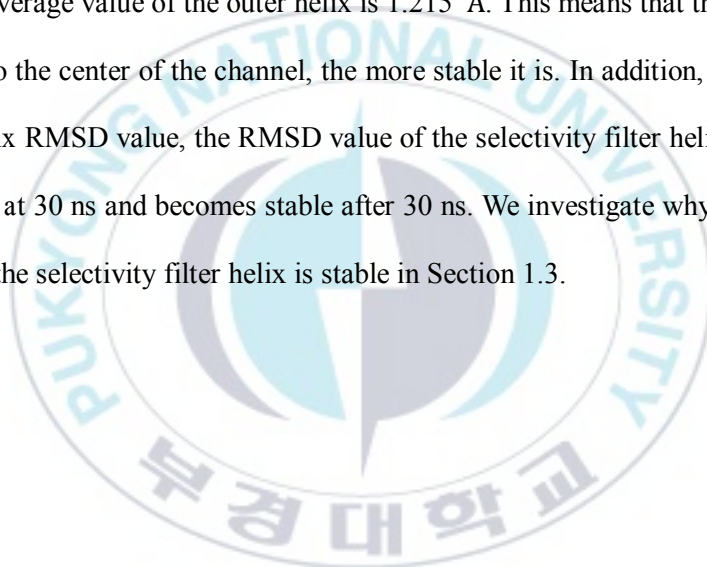
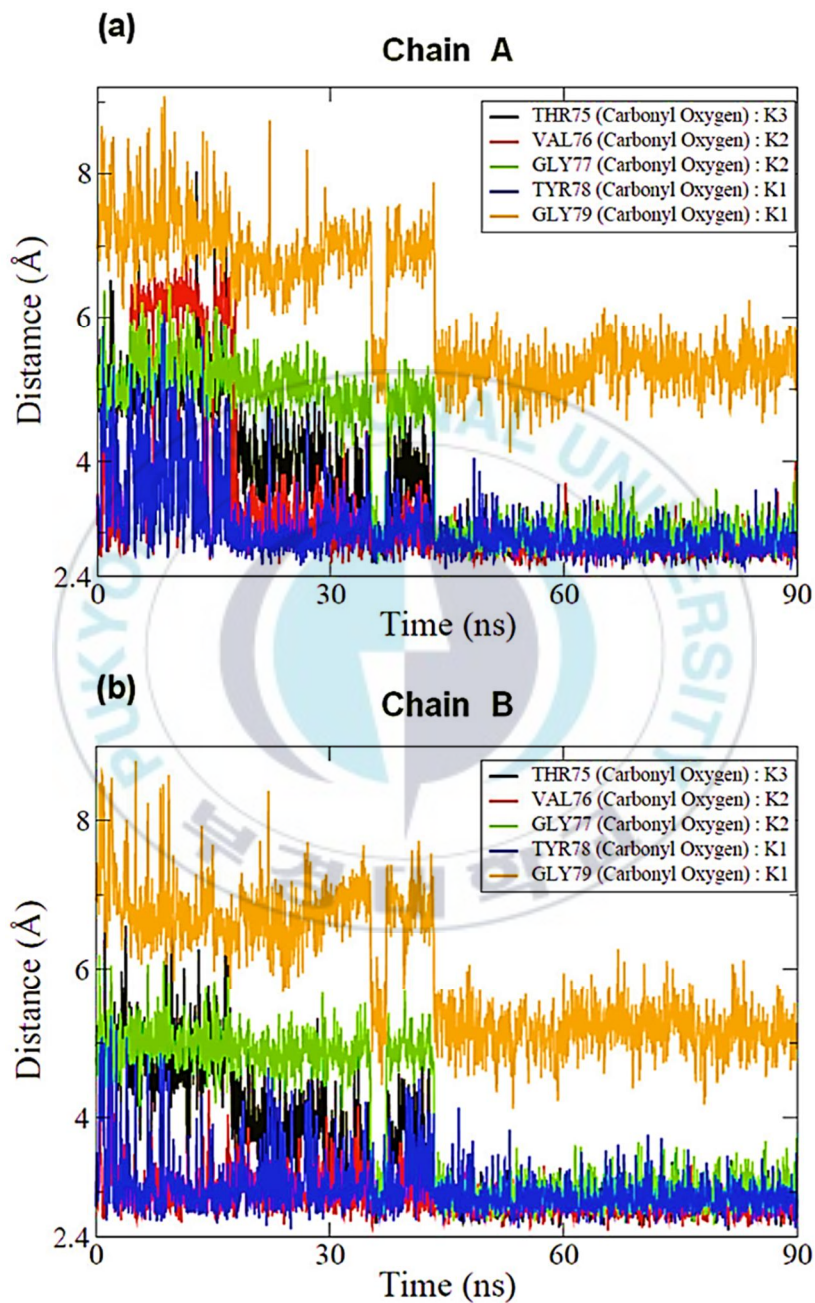


Figure III-2. RMSD of potassium channel: (a) Selectivity filter (b) Pore helix (c) Inner Helix (d) Outer Helix (e) Whole backbone (f) Comparison of all RMSD

We measure RMSD (i.e. routine mean square deviation) for the helical domain of the KcsA channel. Figure III-2 shows the RMSD values of the various helical regions of (a) selectivity filter helix, (b) pore helix, (c) inner helix, (d) outer helix, and (e) whole protein. The red line in from Figure III-2 (a) to (e) represents each mean value. The average value of the selectivity filter helix is 0.384 Å, the average value of the pore helix is 0.531 Å, the average value of the inner helix is 1.403 Å, and the average value of the outer helix is 1.215 Å. This means that the closer the helix is to the center of the channel, the more stable it is. In addition, unlike each other helix RMSD value, the RMSD value of the selectivity filter helix decreases suddenly at 30 ns and becomes stable after 30 ns. We investigate why the RMSD value of the selectivity filter helix is stable in Section 1.3.



1.3. Distance between selectivity filter and potassium ion



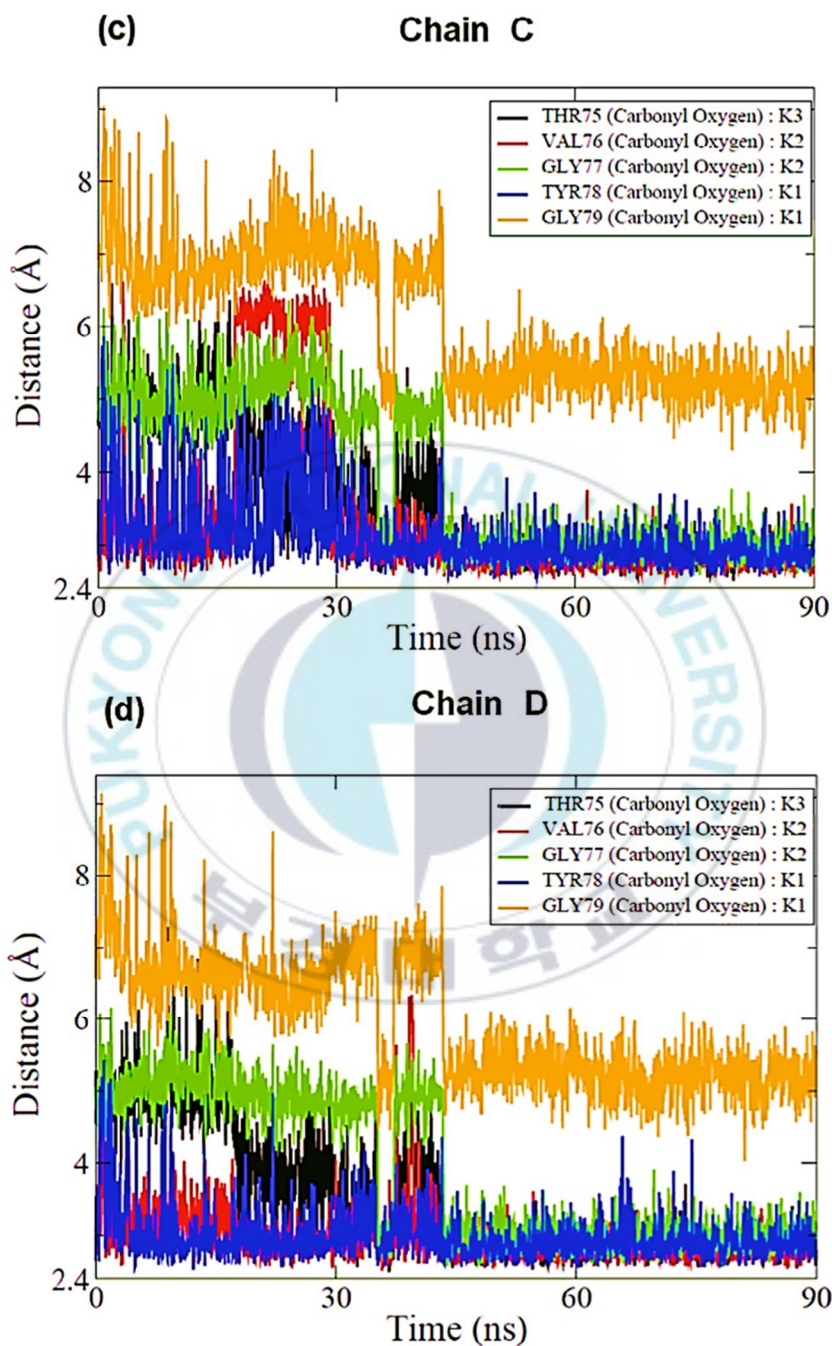


Figure III-3. Distances of three potassium ions (K1, K2, and K3) with respect to Thr75, Val76, Gly77, Tyr78, and Gly79 inside selectivity filter

We measure a distance between potassium ions and water passing through the channels for 90 ns. Since KcsA has a tetramer structure, we expect that each distance from each potassium ion to adjacent residue has the symmetrical length. Measurement results show that the distance values K3 and Thr75's carbonyl oxygen (black) have a very symmetrical pattern; see Figure III-3. One thing we can observe is that all distance values suddenly decrease at 35 ns and then return to the previous values a few nano seconds later. And then it happens again at 43 ns; see Figure III-3. Also, the distance between the carbonyl oxygen and K2 in Val76 (red) and Gly77 (green) changes drastically after 43 ns. Moreover, the distance between K2 ions and Gly77's (green) carbonyl oxygen shows a symmetrical pattern. However, the distance between K2 ions and carbonyl oxygen in Val76 (red) shows an asymmetrical pattern for each chain; see Figure III-3. Let us focus the distance patterns of carbonyl oxygen in K2 ions and Val76 (red) in Figure III-3. We can see that the distances of chains B and D are relatively shorter than those of chains A and C. This means that the position of potassium ion K2 is skewed towards chains B and D, since the position of each chain does not change much. The potassium ion K1 coordinates with carbonyl oxygen of Tyr78 and Gly79; see blue and orange lines in Figure III-3. Commonly, the distance between three potassium ions of the selective filter helix and adjacent residue changes drastically at 43 ns.

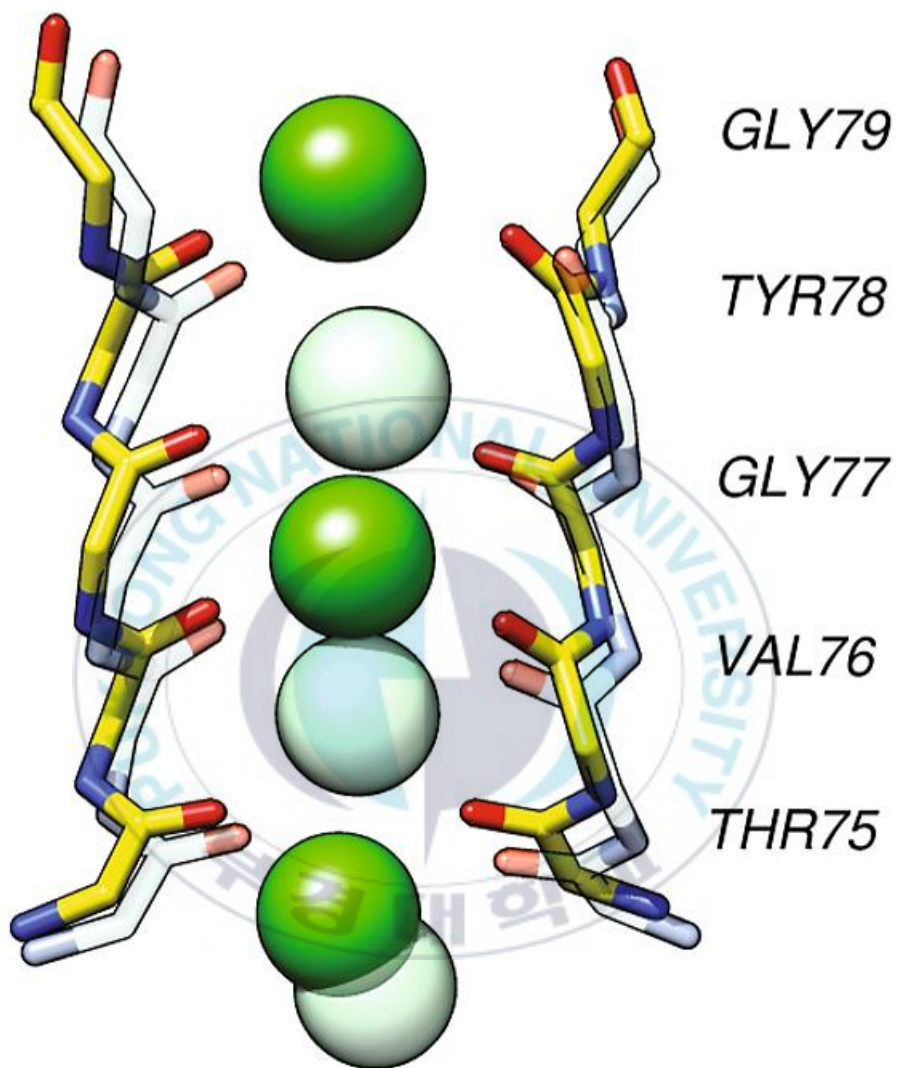
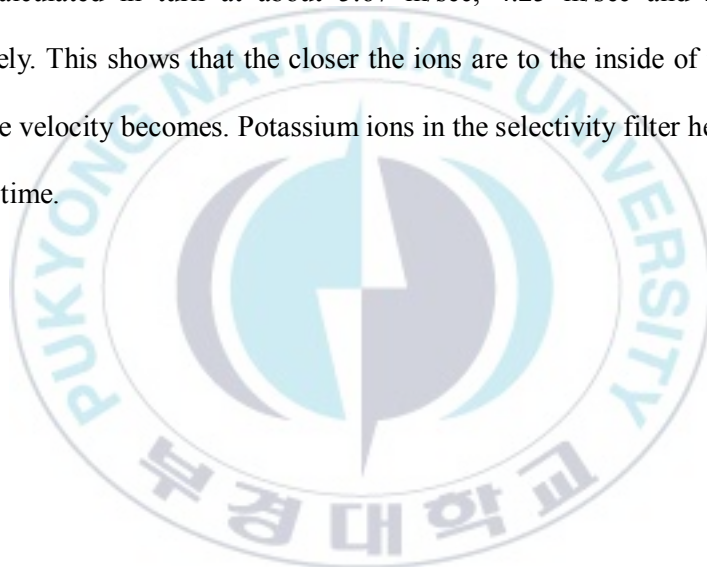
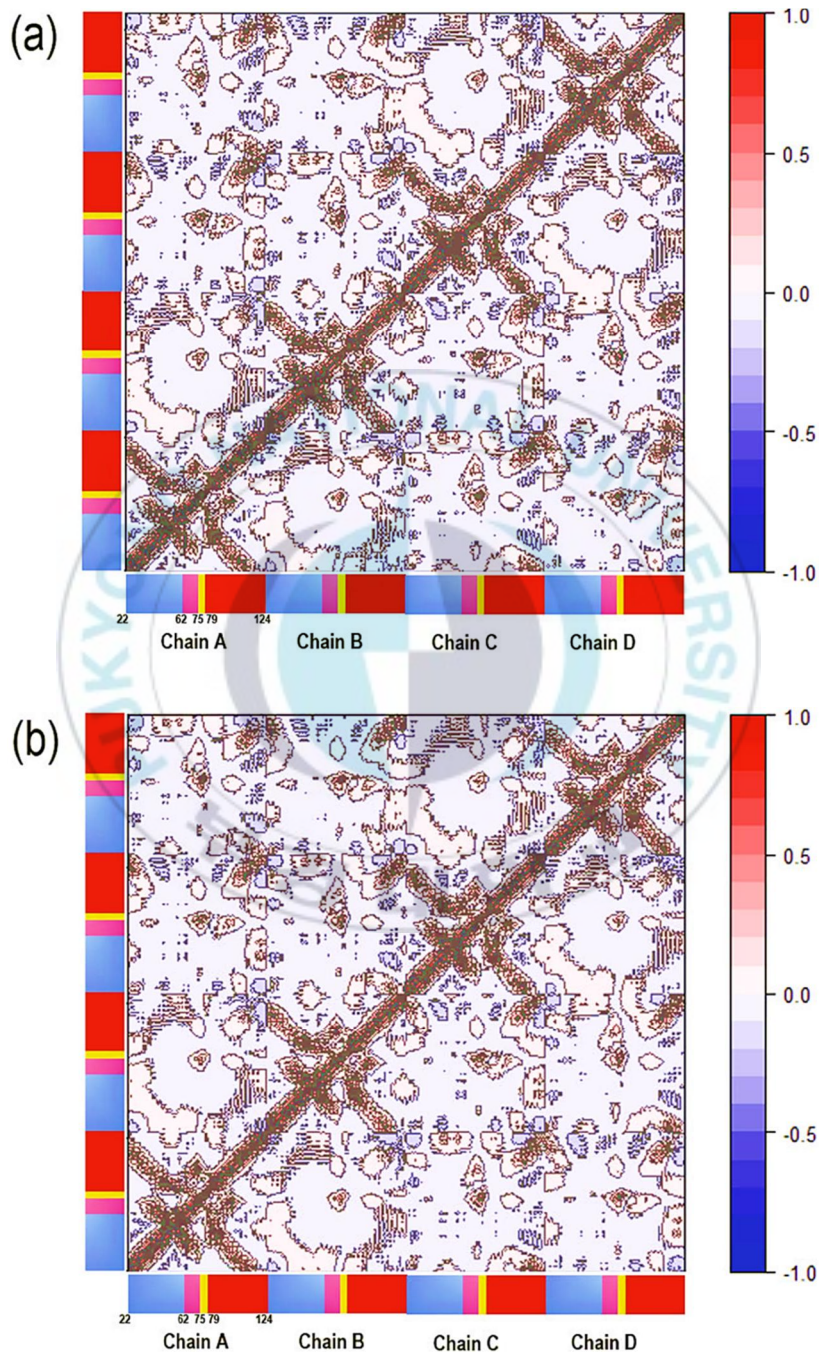


Figure III-4. Snapshots of three potassium ions (K1, K2, and K3) with respect to Thr75, Val76, Gly77, Tyr78, and Gly79 inside selectivity filter at 43.38 ns (Cyan) and 43.44 ns (Green) snapshot. For clarity, waters are not shown

Figure III-4 is compared with two snapshots before and after a sudden change in the distance of potassium ions and adjacent residues. As a result, there is an abrupt movement in the coordinate of potassium ions with adjacent residues at ~43 ns. Figure III-4 shows the relative position of potassium ions before (cyan) and after (green). There is a time interval of 0.06ns. During this time interval, we obtain the velocities of three ions K1, K2 and K3 by using the movement of potassium ions. It was calculated in turn at about 5.67 m/sec, 4.25 m/sec and 2.37 m/sec, respectively. This shows that the closer the ions are to the inside of the cell, the slower the velocity becomes. Potassium ions in the selectivity filter helix move at the same time.



1.4. Correlation map with ion change



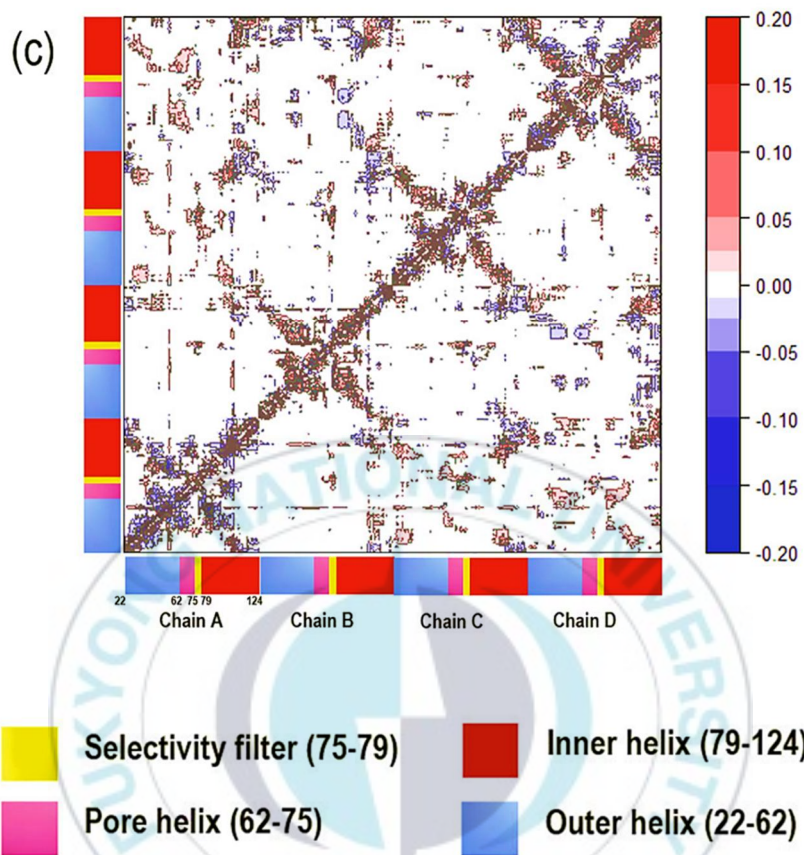


Figure III-5. Correlation map between the two KcsA structures at (a) 43.38 ns, (b) 43.44 ns, (c) the difference between (a) and (b)

In this section, we investigate how potassium ions are affected by the whole area. The correlation of maps (factories) is as follows,

$$C_{ij} = \frac{(r_i(t) - \langle r_i(t) \rangle)(r_j(t) - \langle r_j(t) \rangle)}{\sqrt{(\langle r_i^2(t) \rangle - \langle r_i(t) \rangle^2) - (\langle r_i^2(t) \rangle - \langle r_i(t) \rangle^2)}} \quad (2.33)$$

where $r_i(t)$ and $r_j(t)$ are the atomic locations of that i^{th} and j^{th} C α atoms, receptively at time t . $r_i(t) - \langle r_i(t) \rangle$ corresponds to the fluctuation of i^{th} C α atoms. We use this to obtain correlation maps. Figure III-5 shows correlation maps of the C α atoms (a) before and (b) after these "movement processes", 43.38 ns 43.44 ns respectively.

According to the above equation, the correlation (factor) values are in the range of -1 to +1. These two values mean that they move in the opposite to each other. In other words, positive values mean "correlation movement" between residues, and negative values correspond to "correlational opposite movement" between residues. Figure III-5 (c) shows the transition process before and after. And it can be seen that the correlation of potassium ions is observed throughout the channel protein, not only in certain areas.

In particular, we observe that the inter-domain correlation between chains A and C, and chains A and D shows correlated movements. Conversely, the inter-domain correlations between chains B and C, and chains B and D shows anti-correlated movements. The analysis of correlation maps also suggests that the potassium ion

movement takes place in the same way in the entire region of the channel protein.



1.5. Movement and change of KcsA internal potassium and water molecules

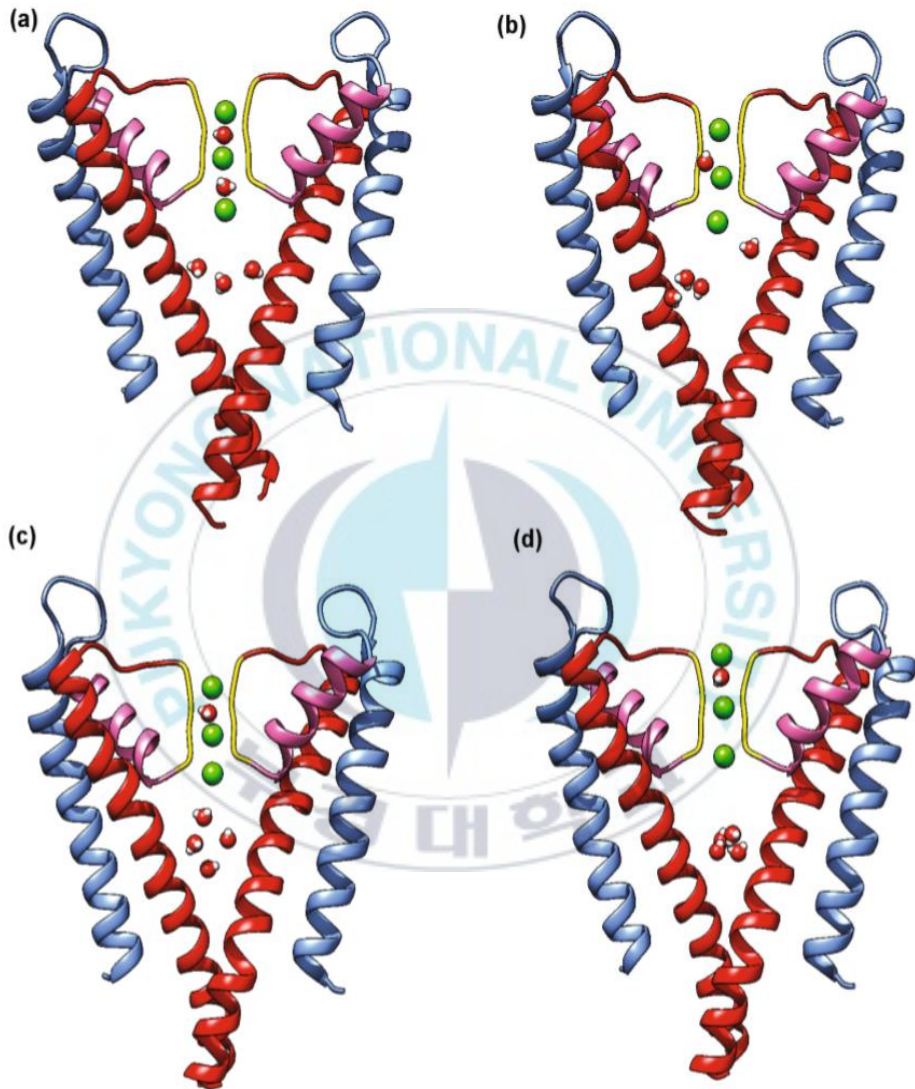


Figure III-6. Movement and change of KcsA internal potassium and water molecules at time (a) 3.6 ns, (b) 17.3 ns, (c) 43.38 ns, and (d) 43.44 ns

In this section, we study the movement of certain water molecules and potassium ions within the selectivity filter helix during 90 ns. Figure III-6 shows the snapshots that we observe the significant movement at time 3.6 ns, 17.3 ns, 43.38 ns, and 43.44 ns, respectively.

The water molecule (W1) between K1 and K2 maintains its position during the movement of potassium ions. When potassium ions rise, the water molecule (W1) also rise; see Figure III-6. On the other hand, since the water molecule (W2) between K2 and K3 appears to be very unstable, then W2 escapes from the selectivity filter during the upward movement of potassium ions. After escaping, W2 does not come back and move to the cluster in a capacity in the channel; see Figure III-6. This is expected that because potassium ions and water molecules are not actively moving, as opposed to the KcsA channel.

IV. Conclusions

Ion channels are the basis of nerve and muscle activities. It is biologically important to observe its structure and dynamics. Especially, KcsA plays a key role in the conduction of potassium ions. Interaction between residues of potassium channels and potassium ions is critical in ensuring high selectivity for the rapid and passive diffusion of potassium ions. We studied the movement of ions in a channel in a certain environment.

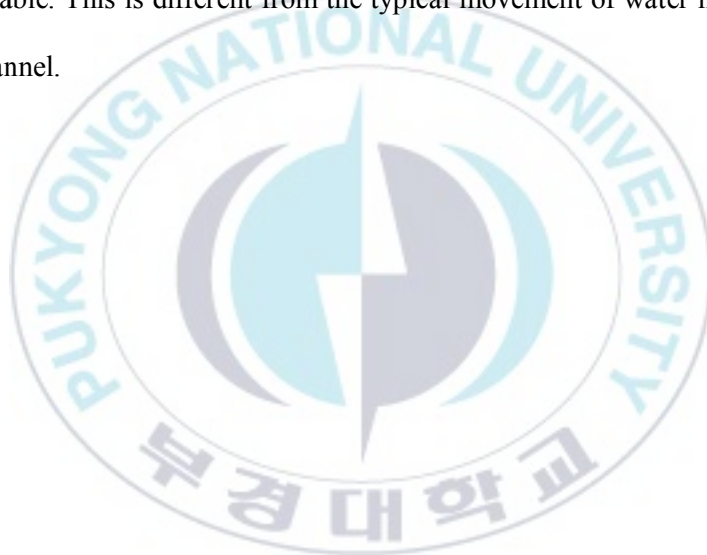
We performed molecular dynamics (MD) simulations to observe the moving of potassium ion with high concentration system. Also MD simulation is an interface between theory and experiment. We have created a 400mM KCL system with no membrane potential.

We modified KcsA channel structure that three potassium ions and two water molecules are aligned alternatively. Also, we measured RMSDs for helix domains of KcsA channel. RMSDs is more stable as it was close to the pore. Moreover, we investigated the distances of potassium ions and residues of the selectivity filter helix for tetramer chains. Potassium ions move up and down simultaneously on the channel and the distance of potassium decreases suddenly at 43 ns.

We found that the sudden changes were because of the movement of potassium

ions about 43 ns. The closer to the inside of the cell, the slower the velocity of potassium ions. We looked at the correlation for all C α atoms undergoing the changes from 43.38 ns and 43.44 ns. There are correlations across KcsA channels, not specific regions.

Moreover, we examined how the water molecules in KcsA channel move in a certain time. Water molecule (W1) rises with ions, but water molecule (W2) is very unstable. This is different from the typical movement of water molecules in KcsA channel.



Reference

- [1] Nelson, D. L., Lehninger, A. L., & Cox, M. M. (2008). *Lehninger principles of biochemistry*. Macmillan.
- [2] Ramachandran, G. N. (1963). Stereochemistry of polypeptide chain configurations. *J. Mol. Biol.*, 7, 95-99.
- [3] Ramachandran, G. T., & Sasisekharan, V. (1968). Conformation of polypeptides and proteins. In *Advances in protein chemistry* (Vol. 23, pp. 283-437). Academic Press.
- [4] Shrivastava, I. H., & Bahar, I. (2006). Common mechanism of pore opening shared by five different potassium channels. *Biophysical Journal*, 90(11), 3929-3940.
- [5] Jiang, Y., Lee, A., Chen, J., Cadene, M., Chait, B. T., & MacKinnon, R. (2002). The open pore conformation of potassium channels. *Nature*, 417(6888), 523.
- [6] Zhou, Y., Morais-Cabral, J. H., Kaufman, A., & MacKinnon, R. (2001). Chemistry of ion coordination and hydration revealed by a K⁺ channel-Fab complex at 2.0 Å resolution. *Nature*, 414(6859), 43.
- [7] Lee, B., & Richards, F. M. (1971). The interpretation of protein structures: estimation of static accessibility. *Journal of molecular biology*, 55(3), 379-414.
- [8] Kuo, A., Gulbis, J. M., Antcliff, J. F., Rahman, T., Lowe, E. D., Zimmer, J., ... & Doyle, D. A. (2003). Crystal structure of the potassium channel KirBac1.1 in the closed state. *Science*, 300(5627), 1922-1926.
- [9] Bernèche, S., & Roux, B. (2005). A gate in the selectivity filter of potassium channels. *Structure*, 13(4), 591-600.
- [10] Imai, S., Osawa, M., Takeuchi, K., & Shimada, I. (2010). Structural basis underlying the dual gate properties of KcsA. *Proceedings of the National Academy of Sciences*, 107(14), 6216-6221.
- [11] Miloshevsky, G. V., & Jordan, P. C. (2008). Conformational changes in the selectivity filter of the open-state KcsA channel: an energy minimization study. *Biophysical*

- journal*, 95(7), 3239-3251.
- [12] Shimizu, H., Iwamoto, M., Konno, T., Nihei, A., Sasaki, Y. C., & Oiki, S. (2008). Global twisting motion of single molecular KcsA potassium channel upon gating. *Cell*, 132(1), 67-78.
- [13] Compoin, M., Carloni, P., Ramseyer, C., & Girardet, C. (2004). Molecular dynamics study of the KcsA channel at 2.0-Å resolution: stability and concerted motions within the pore. *Biochimica et Biophysica Acta (BBA)-Biomembranes*, 1661(1), 26-39.
- [14] Berneche, S., & Roux, B. (2000). Molecular dynamics of the KcsA K⁺ channel in a bilayer membrane. *Biophysical journal*, 78(6), 2900-2917.
- [15] Allen, T. W., Kuyucak, S., & Chung, S. H. (1999). Molecular dynamics study of the KcsA potassium channel. *Biophysical journal*, 77(5), 2502-2516.
- [16] Shrivastava, I. H., & Sansom, M. S. (2000). Simulations of ion permeation through a potassium channel: molecular dynamics of KcsA in a phospholipid bilayer. *Biophysical Journal*, 78(2), 557-570.
- [17] Capener, C. E., Shrivastava, I. H., Ranatunga, K. M., Forrest, L. R., Smith, G. R., & Sansom, M. S. (2000). Homology modeling and molecular dynamics simulation studies of an inward rectifier potassium channel. *Biophysical journal*, 78(6), 2929-2942.
- [18] Compoin, M., Carloni, P., Ramseyer, C., & Girardet, C. (2004). Molecular dynamics study of the KcsA channel at 2.0-Å resolution: stability and concerted motions within the pore. *Biochimica et Biophysica Acta (BBA)-Biomembranes*, 1661(1), 26-39.
- [19] Shrivastava, I. H., Tieleman, D. P., Biggin, P. C., & Sansom, M. S. (2002). K⁺ versus Na⁺ ions in a K channel selectivity filter: a simulation study. *Biophysical journal*, 83(2), 633-645.
- [20] Lu, T., Ting, A. Y., Mainland, J., Jan, L. Y., Schultz, P. G., & Yang, J. (2001). Probing ion permeation and gating in a K⁺ channel with backbone mutations in the selectivity filter. *Nature neuroscience*, 4(3), 239.

- [21] Luzhkov, V. B., & Åqvist, J. (2000). A computational study of ion binding and protonation states in the KcsA potassium channel. *Biochimica et Biophysica Acta (BBA)-Protein Structure and Molecular Enzymology*, 1481(2), 360-370.
- [22] Zhou, Y., & MacKinnon, R. (2003). The occupancy of ions in the K⁺ selectivity filter: charge balance and coupling of ion binding to a protein conformational change underlie high conduction rates. *Journal of molecular biology*, 333(5), 965-975.
- [23] Morais-Cabral, J. H., Zhou, Y., & MacKinnon, R. (2001). Energetic optimization of ion conduction rate by the K⁺ selectivity filter. *Nature*, 414(6859), 37.
- [24] Leach, A. R., & Leach, A. R. (2001). *Molecular modelling: principles and applications*. Pearson education.
- [25] Frenkel, D., & Smit, B. (2001). *Understanding molecular simulation: from algorithms to applications* (Vol. 1). Elsevier.
- [26] Phillips, J. C., Braun, R., Wang, W., Gumbart, J., Tajkhorshid, E., Villa, E., ... & Schulten, K. (2005). Scalable molecular dynamics with NAMD. *Journal of computational chemistry*, 26(16), 1781-1802.
- [27] MacKerell Jr, A. D. (2004). Empirical force fields for biological macromolecules: overview and issues. *Journal of computational chemistry*, 25(13), 1584-1604.
- [28] Darden, T., York, D., & Pedersen, L. (1993). Particle mesh Ewald: An N · log (N) method for Ewald sums in large systems. *The Journal of chemical physics*, 98(12), 10089-10092.
- [29] Darden, T. A., Pedersen, L. G., Toukmaji, A., Crowley, M., & Cheatham, T. (1997, March). Particle-Mesh Based Methods for Fast Ewald Summation in Molecular Dynamics Simulations. In *PPSC*.
- [30] Essmann, U., Perera, L., Berkowitz, M. L., Darden, T., Lee, H., & Pedersen, L. G. (1995). A smooth particle mesh Ewald method. *The Journal of chemical physics*, 103(19), 8577-8593.

- [31] York, D., & Yang, W. (1994). The fast Fourier Poisson method for calculating Ewald sums. *The Journal of Chemical Physics*, 101(4), 3298-3300.
- [32] Petersen, H. G. (1995). Accuracy and efficiency of the particle mesh Ewald method. *The Journal of chemical physics*, 103(9), 3668-3679.
- [33] Martyna, G. J., Tobias, D. J., & Klein, M. L. (1994). Constant pressure molecular dynamics algorithms. *The Journal of Chemical Physics*, 101(5), 4177-4189.
- [34] Andrew, R. L. (2001). Molecular modeling principles and applications. 2nd, editor.: Pearson Education Limited.
- [35] Frenkel, D., & Smit, B. (2001). *Understanding molecular simulation: from algorithms to applications* (Vol. 1). Elsevier.
- [36] Berendsen, H. J., Postma, J. V., van Gunsteren, W. F., DiNola, A. R. H. J., & Haak, J. R. (1984). Molecular dynamics with coupling to an external bath. *The Journal of chemical physics*, 81(8), 3684-3690.

Acknowledgement

2년이라는 시간이 빠르게 흘러 석사 졸업을 앞두고 있습니다. 새로운 시작에 생소하고 어려운 부분이 많았음에도, 언제나 도와주시고 보다 더 나은 방향으로 이끌어 주신 이상욱 지도 교수님께 진심으로 감사한 마음을 전합니다. 제가 배우는 영역은 여태 공부해 온 것과 다르고 처음 접하는 여러 프로그램 사용에 있어 혼란스러운 부분이 많았습니다. 아직 많이 부족하지만 성취감도 느낄 수 있었고, 스스로 문제를 해결하는 방법에 대해 공부할 수도 있었습니다. 또 더 노력했다면, 더 잘해낼 수 있지 않았을까 하는 아쉬움도 함께 남는 시간이었습니다.

석사 생활에 있어서 언제나 격려와 관심을 주시는 장재원 교수님과 남승일 교수님, 또 한국외국어대학교 화학과 은창선 교수님께도 감사의 말씀을 전합니다. 교수님들의 조언과 지도 덕분에 보다 발전할 수 있었습니다.

돌이켜 보면 혼자서 해결할 수 없는 어려운 일이 많았습니다. 같은 실험실에서 저에게 부족한 부분을 채워주며 함께 생활했던 현정이 언니, 수진이 언니, 수현이, 수지, 지원이에게도 고마움을 느낍니다. 선배들의 조언 및 도움이 없었더라면 더 힘들었을 것이라고 생각합니다. 또한 제 연구에 있어 도움을 주고 격려해준 Jayaraman에게도 고맙다고 전하고 싶습니다.

마지막으로 저를 항상 사랑해주고 지지해주는 가족들에게도 진심으로 감사하다는 말을 전하며 글을 마칩니다. 이렇게 많은 분들의 관심과 격려 덕분에 한 단계 더 나아간 저를 느낄 수 있습니다. 이 논문이 완성되기까지 도움을 주셨던 모든 분들께 다시 한 번 감사 드립니다.

2019년 8월

김 묘 정